Optical cooling of single-walled carbon nanotubes as revealed by their anti-Stokes Raman spectra

2008 J. Phys.: Condens. Matter 20 275215

(http://iopscience.iop.org/0953-8984/20/27/275215)

J. Phys.: Condens. Matter **20** (2008) 275215 (7pp) doi:10.1088/0953-8984/20/27/275215

Optical cooling of single-walled carbon nanotubes as revealed by their anti-Stokes Raman spectra

I Baltog[1], **M Baibarac**[1] **and S Lefrant**[2]

[1] National Institute of Materials Physics, Laboratory of Optics and Spectroscopy, Bucharest, PO Box MG-7, R-76900, Romania
[2] Institut des Matériaux de Nantes, Laboratoire des Materiaux et Nanostructures, 2 rue de la Houssinière, BP 32229, 44322 Nantes, France

Received 29 January 2008, in final form 2 May 2008
Published 4 June 2008
Online at stacks.iop.org/JPhysCM/20/275215

Abstract

Semiconducting single-walled carbon nanotubes resonantly excited by the interband E_{22}^{S} electronic transitions (at 1064 nm) display for the two components of the radial Raman band—one associated with the isolated tubes and the other associated with the bundled tubes—an anti-Stokes/Stokes Raman intensity ratio (I_{aS}/I_{S}) which deviates oppositely from the predictions of the Maxwell–Boltzmann formula. A cooling and heating vibration process, evidenced by an enhancement and diminishment of (I_{aS}/I_{S}), appears in the isolated and bundled nanotubes, respectively. Here we confirm a cooling process, observed only for semiconducting nanotubes, which emerges from the relaxation of the E_{22}^{S} excited state by the electronic relaxation from E_{22}^{S} to E_{11}^{S} that precedes the spontaneous luminescence emission at E_{11}^{S}. Metallic nanotubes do not exhibit luminescence and no cooling effect is observed. Both semiconducting and metallic nanotubes show for the bundled component of the radial Raman band an enhancement of (I_{aS}/I_{S}) such as is frequently observed in a coherent anti-Stokes Raman scattering process.

(Some figures in this article are in colour only in the electronic version)

1. Introduction

Raman scattering has been widely used to characterize single-walled carbon nanotubes (SWNTs) [1–3]. The Raman spectra exhibit three main groups of bands whose relative intensities and peak positions vary with the excitation wavelengths. A first group, ranging from 100 to 350 cm^{-1}, is associated with the radial breathing modes (RBM). It is generally accepted that the radial band associated with a specific (n, m) nanotube comprises two components, one associated with the isolated tubes (I_{single}) and the other, upshifted by $\approx$14 cm^{-1}, with the bundled tubes (I_{bundle}). The RBM peak position (Ω cm^{-1}) value and the equation $\Omega(cm^{-1}) = 223.75/d$ (nm) provides an efficient method for determining the diameters (d) of the isolated tubes (I_{single}). The Raman signature of bundled tubes (I_{bundle}) is a weaker band appearing as a shoulder of the RBM line associated with the isolated tubes. The bundled tube's diameter can be estimated from the RBM frequency using several expressions, one of these being Ω (cm^{-1}) = 223.75 (nm cm^{-1})/d (nm) + $\Delta\Omega$ (cm^{-1}), where $\Delta\Omega$ = 14 cm^{-1} denotes the upshift due to tube–tube interaction [4, 5]. Bands belonging to this group are very sensitive to the excitation wavelength; their intensity is much enhanced when the photon energy of the excitation light corresponds to a transition between the van Hove singularities (E_{ii}) in the valence and conduction bands of all possible nanotubes [1–3].

In the interval from 1100 to 1700 cm^{-1} two bands are found: a broad one aligned in the 1500–1600 cm^{-1} range, labeled the G band, is associated with the tangential stretching modes (TM). Another, frequently referred to as the 'D band', is not intrinsically related to the nanotube structure—it is also present in the Raman spectrum of graphitic materials. As a general rule, the intensity of the D band is indicative of disorder induced in the graphitic lattice or defects in nanotubes. A distinguishing feature of the G bands, related to the contribution of the metallic nanotubes, is a new component with a maximum at $\sim$1540 cm^{-1} that appears at laser excitation

energies of 1.7–2.2 eV. This wide band, asymmetric towards lower frequencies, fits a Breit–Wigner–Fano (BWF) profile which indicates electron–phonon type interactions [1–3].

The third group, located in the high frequency range from 1700 to 3500 cm^{-1}, corresponds to the second-order Raman spectrum. As a rule, the most intense bands are those detected at approximately twice the frequency of the D and G bands.

In the Raman studies of carbon nanotubes much attention has been paid to an unusual anti-Stokes Raman effect characterized by an abnormal intensity, sometimes increasing with the vibration wavenumber, large differences of line profiles on Stokes Raman (SR) and anti-Stokes Raman (aSR) sides and some discrepancies between the Stokes and anti-Stokes frequencies [1–3].

High values of the anti-Stokes/Stokes intensity ratio (I_{aS}/I_S) and different line shapes of the G band are the most characteristic reported features. A number of different interpretations have been given for the asymmetry of the SR and aSR spectra of SWNTs: (i) as resulting from a doubly resonant Raman scattering effect produced by the excitation of different (n, m) nanotubes with the incident and Stokes scattered photons [6–8]; (ii) as indicative of the non-thermal overpopulation of the higher vibration states generated by the large photon density of the excitation light combined with an enhancement of the Raman cross section [9]; (iii) as resulting from nonlinear optical processes [10, 11]. In the last case, as a general rule, the abnormal aSR emission has not to be uniquely related with SWNTs. Indeed, this phenomenon has been observed in other materials when these have been subjected to light scattering experiments in which the energy of the excitation light has coincided with the energy of an electronic transition. Here, the third-order dielectric susceptibility becomes different to zero, $\chi^{(3)} \neq 0$, which is the necessary requirement for the generation of nonlinear optical processes. Recently, this has been the basis for accurate identification of an abnormal aSR emission as having the characteristics of coherent anti-Stokes Raman scattering (CARS) for different materials such as SWNTs, double-walled carbon nanotubes, glassy carbon, copper phthalocyanine and poly(bithiophene) [10, 11]. Normally, at resonant excitation when $\chi^{(3)} \neq 0$, the abnormal aSR emission generated by a CARS process is observed for all lines of the Raman spectrum, its intensity varying with the square of the exciting laser intensity, film thickness and Raman shift Ω [10, 11].

Returning to the SWNTs it should be pointed out that most of the anti-Stokes Raman studies have been focused on the behavior of the Raman bands situated in the interval from 1100 to 1700 cm^{-1}, i.e., where the D and G bands are found, and little attention has been paid to the bands associated with the radial breathing modes (RBM). For the nanotubes of a distinct diameter, when the photon energy of the excitation light corresponds to a transition between the van Hove singularities (E_{ii}) the intensity of RBM is much enhanced [1–3].

Such a situation is encountered for the SWNTs of about 1.35 nm diameter for which the laser excitation light of 676.4 and 1064 nm produces an interband transition between the E_{11}^M and E_{22}^S van Hove singularities of metallic and semiconducting nanotubes, respectively [1–3]. Once excited, the metallic and semiconducting nanotubes return directly and indirectly to the ground state. For the latter tubes other radiative processes are observed simultaneously with the Raman scattering. Hot luminescence and relaxed fluorescence are the main phenomena that may occur when the system exchanges energy with its environment [12]. The redistribution of the optical absorbed energy among the system's excited states before it de-excites by luminescence implies a supplementary depopulation of the upper vibration levels of the electronic excited state through mechanisms other than spontaneous Raman scattering. This manifests itself as a cooling of the system.

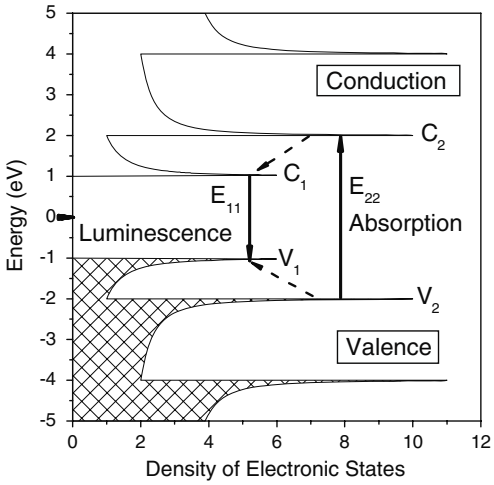

Figure 1. Scheme of the luminescence emission from the E_{11}^S state of semiconducting SWNTs populated by the phonon relaxation of the optical E_{22}^S excited level.

As in [13], figure 1 illustrates another de-excitation mode for the E_{22}^S state by the electronic relaxation from E_{22}^S to E_{11}^S followed up by the luminescence emission at E_{11}^S. In these conditions, due to the supplementary depopulation of the upper vibration levels of the E_{22}^S electronic excited state, the Maxwell–Boltzmann (M–B) law:

$$\frac{I_{\text{anti-Stokes}}}{I_{\text{Stokes}}} = \left(\frac{\omega_0 - \Omega}{\omega_0 + \Omega}\right)^4 \exp\left(\frac{h\Omega}{kT}\right)^{-1} \qquad (1)$$

no longer applies. Thus, the aSR intensity deviates from that predicted by the M–B formula; it becomes weaker as a result of supplementary depletion of the E_{22}^S state due to the transition towards E_{11}^S. Such a phenomenon has to be quite similar to that observed for isolated atoms and molecules under resonant optical excitation [14]. In semiconducting materials, the excitonic resonance substitutes the atomic resonance [15]. Due to quantum confinement, the electronic density of the nanometric systems, for example the van Hove singularities of carbon nanotubes [1–3], are characterized by very thin levels, which could be involved in generation of a quantum cooling process. At a fixed sample temperature, the population of the E_{11}^S electronic level is accomplished by the electronic transition $E_{22}^S \rightarrow E_{11}^S$ resulting in a depletion of the former level. Thereafter, the Raman scattering process at the E_{22}^S occurs in conditions of an underpopulation of the respective

electronic level. In this context, the I_{aS}/I_S ratio associated with the isolated component of the Raman band associated with the RBM must be smaller than that prescribed by the M–B law.

The equation (1), where ω_0, Ω, h, k and T are the excitation light frequency, the wavenumber of the Raman line (cm^{-1}), the Planck constant, the Boltzmann constant and the temperature, respectively, is entirely applicable in the case of the metallic nanotubes which return directly to the ground state of the E_{11}^M level.

This current work seeks to demonstrate experimentally this particular behavior of the anti-Stokes Raman spectra associated with radial breathing modes (RBM) of semiconducting and metallic nanotubes when they are resonantly excited by the transitions E_{22}^S and E_{11}^M, respectively. The smaller than predicted value of I_{aS}/I_S observed for the radial Raman bands of isolated semiconducting SWNTs at thermal equilibrium is interpreted as resulting from an optical cooling process occurring via the transition $E_{22}^S \rightarrow E_{11}^S$ as an additional depletion route of the E_{22}^S state. It is interesting to note that such a phenomenon illustrating an optical cooling of the SWNTs has not been previously observed.

2. Experimental details

We have used SWNTs of about 1.35 nm diameter produced by arc discharge [16, 17] and chemical vapor deposition (ALDRICH) techniques. They are resonantly excited by laser light of 676.4 and 1064 nm that supply the transitions in the states E_{11}^M and E_{22}^S of metallic and semiconducting nanotubes respectively. Raman spectra were obtained using the surface enhanced Raman scattering (SERS) technique. SERS spectra were recorded in backscattering geometry, in air, using a Jobin Yvon T64000 Raman spectrophotometer and a Bruker RFS 100 FT Raman spectrophotometer, respectively. Both spectrophotometers were fitted with a microprobe allowing the laser light to be focused to a dot on the sample with micrometer accuracy. A microscope objective of 0.55 numerical aperture was used. The Stokes and anti-Stokes pair spectra were recorded under the same conditions. We used films of about 150 nm thickness deposited on a SERS active support. SWNTs films were obtained by evaporating a solvent (toluene) from a uniformly distributed emulsion of nanotubes on rough Au substrates. Gold SERS active substrates, with a mean roughness of about 30–100 nm, were prepared by the vacuum evaporation [18].

3. Results and discussion

The Raman bands associated with RBM are very sensitive to the excitation wavelength. At resonance, i.e. when the photon energy of the excitation light corresponds to a transition between the van Hove singularities (E_{ii}) in the valence and conduction bands of a distinct nanotube, the intensity of the RBM is much enhanced. Assuming a thermal equilibrium state, the whole structure of the Raman bands associated with the RBM, formed by the contribution of isolated and bundled tubes, can be described in the aSR side by equation (1). Figure 2 presents the SR and aSR

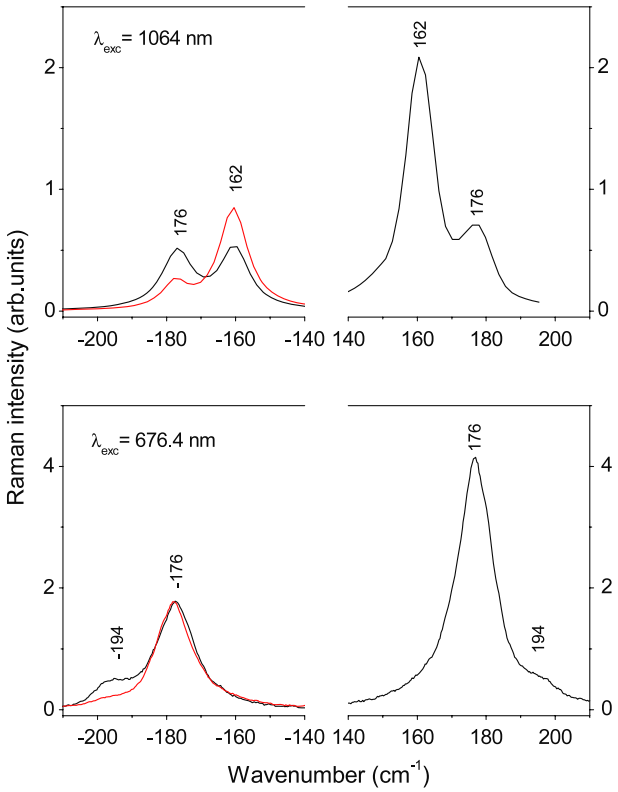

Figure 2. Stokes and anti-Stokes micro-SERS spectra of SWNTs at $\lambda_{exc} = 1064$ nm and 676.4 nm with 25 mW exciting light power focused onto a spot area of about 1 μm^2. The red curves, showing a lower intensity for bands at -176 and -194 cm^{-1}, represent the anti-Stokes spectra calculated applying the Maxwell–Boltzmann formula to the Stokes spectra. Thin films of SWNTs (about 50 nm thickness) were deposited on gold substrates with a mean roughness of about 150 nm.

spectra associated with the RBM of SWNTs of about 1.35 nm diameter at the laser excitation wavelengths of 1064 and 676.4 nm which activate the E_{22}^S and E_{11}^M interband transitions between the van Hove singularities of semiconducting and metallic nanotubes, respectively [1–3]. For the semiconducting nanotubes, revealed by the excitation with 1064 nm, the two components of the RBM band, I_{single} ($\sim$162 cm^{-1}) and I_{bundle} ($\sim$176 cm^{-1}), behave differently on the anti-Stokes side than the theoretical expectations based on thermal equilibrium; I_{single} exhibits a diminishment while the I_{bundle} shows an enhancement. The same SWNT samples under laser light of 676.4 nm, that ensures the resonant excitation of metallic nanotubes, display I_{single} at $\sim$176 cm^{-1} whose anti-Stokes replica entirely coincides with that calculated using the M–B formula. We find that for the metallic nanotubes, I_{bundle} at about 194 cm^{-1} appears as a shoulder whose intensity on the anti-Stokes side increases almost quadratically with the film thickness and exciting laser intensity. Such a result is intriguing. At thermal equilibrium, the (I_{aS}/I_S) ratio must reflect the temperature dependence of the relative phonon populations. In these conditions, if an eventual change of the sample temperature under focused laser light takes place, then the I_{aS}/I_s ratio is predicted to vary in a similar fashion and in the same sense for both components of the radial bands, I_{single}

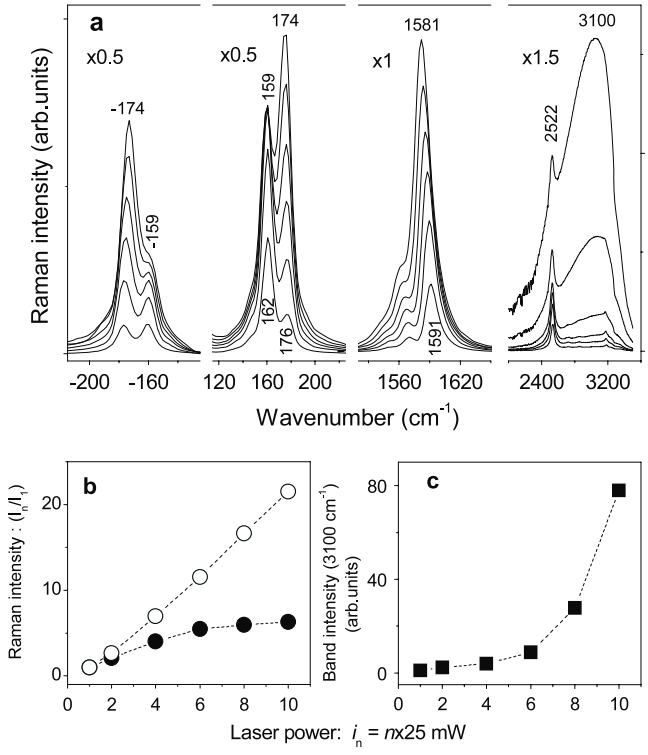

Figure 3. (a) Micro-SERS spectra of SWNTs at $\lambda_{exc} = 1064$ nm under different laser excitation powers (from bottom to top: 25, 50, 100, 150, 200 and 250 mW) focused onto a spot (area about 1 μm^2) of the sample. (b) The growth in the anti-Stokes side of the Raman spectra associated with the RBM of isolated nanotubes, I_{single} (full circle), and bundled nanotubes, I_{bundle} (open circle). (c) The growth with the laser exciting power of the wide band at ∼3100 cm^{-1} (full square).

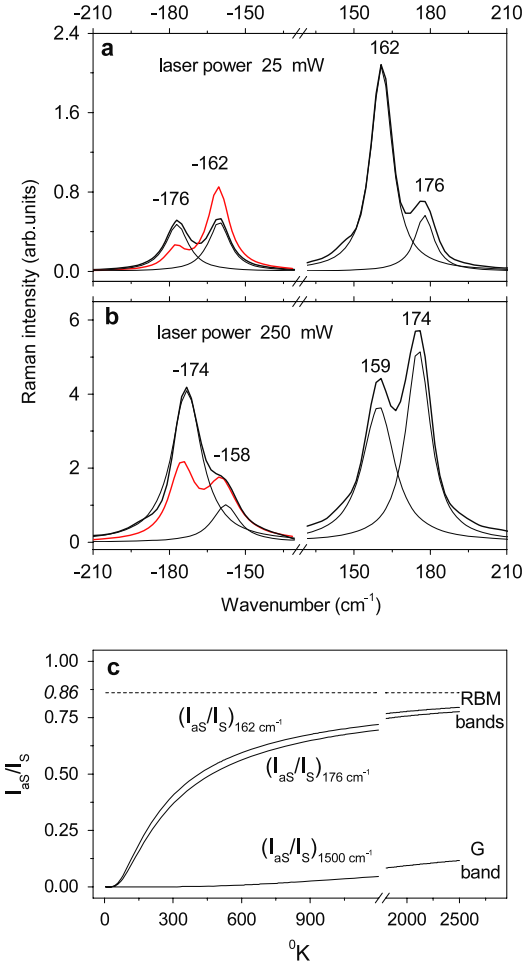

Figure 4. Stokes and anti-Stokes micro-SERS spectra of SWNTs at $\lambda_{exc} = 1064$ nm and two powers of 25 mW (a) and 250 mW (b) focused onto a spot area of about 1 μm^2. The red curves, showing a lower intensity for bands at −176 and −174 cm^{-1}, represent the anti-Stokes spectra calculated applying the Maxwell–Boltzmann formula to the Stokes spectra. In (c) we present the variation of the I_{aS}/I_S intensity ratio for the Raman lines associated with RBM (162 and 176 cm^{-1}) for the isolated (162 cm^{-1}) and bundled tubes (176 cm^{-1}) and tangential vibration modes (G band) calculated with the Maxwell–Boltzmann formula.

and I_{bundle}, regardless of the tube nature, i.e., semiconducting or metallic. Such a scenario cannot explain why the same sample shows on the anti-Stokes side a different behavior for the Raman bands associated with the isolated (I_{single}) and bundled (I_{bundle}) nanotubes, semiconducting and metallic.

The question is thought-provoking, looking at figure 3 where the abnormal I_{aS}/I_s ratio of I_{single} and I_{bundle} is still present in the Raman spectra of SWNTs at $\lambda_{exc} = 1064$ nm when the power of the laser exciting light is varied between 25 and 250 mW. In this case, due to a warming process developed in the micron focused area of the investigated sample, all Raman lines downshift at ∼0.994 Ω. This means a translation of about 2 cm^{-1} for the RBM and 10 cm^{-1} for the G band, which is in agreement with other reported experiments in which the sample temperature was increased up to ∼6000 K [19–21]. Contrary to expectation, figure 3(a) shows a different variation in the aSR side of I_{bundle} and I_{single}, the former increasing two times faster. Worth noticing is that on the aSR side I_{single} is always weaker while I_{bundle} is more intense than the values predicted by the M–B formula. The variations in the aSR side against the laser exciting power of I_{single} and I_{bundle} are summarized in figure 3(b). Clearly, the two components of RBM increase differently with the laser intensity, I_{bundle} two times faster than I_{single}. For the new band peaking at ∼3100 cm^{-1} an exponential growth is observed; figure 3(c). These variations are quite reversible as the laser intensity ($\lambda_{exc} = 1064$ nm) is increased and decreased, so permanent thermal modification of SWNTs cannot be considered; for an explanation of the anomaly in the I_{aS}/I_S ratio behavior as well as the appearance of the new emission band at ∼3100 cm^{-1} other physical processes have to be considered.

Figures 4(a) and (b) detail the Stokes and anti-Stokes SWNTs SERS spectra at $\lambda_{exc} = 1064$ nm under two light exciting power levels, 25 and 250 mW. The dashed curves represent the aSR spectra as calculated by applying the M–B formula to the SR spectrum, and the thin continuous graphs represent the two deconvoluted radial components, I_{single} and I_{bundle}. At thermal equilibrium, when the M–B law operates, the I_{aS}/I_S ratios of different Raman bands, I_{single}, I_{bundle} and I_G, vary as shown in figure 4(c). Clearly, the I_{aS}/I_S ratio of Raman bands associated with the two components of RBM

Table 1. The I_{aS}/I_S intensity ratio of Raman lines associated with RBM (I_{single} and I_{bundle}) for SWNTs as a function of temperature ($\lambda_{exc} = 1064$ nm) and film thickness ($\lambda_{exc} = 676.4$ nm). Experimental and theoretical values (calculated by M–B formula).

Temperature effect on the I_{aS}/I_S ratio of Raman bands associated with RBM of semiconducting SWNTs					
Laser power (mW) at $\lambda_{exc} = 1064$ nm corresponding to the E_{22}^S resonant level excitation of semiconducting SWNTs	Estimated temperature taking into account the downshift of the Stokes–Raman bands (K)	I_{aS}/I_S ratio associated with I_{single} of semiconducting RBM (161 cm^{-1})		I_{aS}/I_S ratio associated with I_{bundle} of semiconducting RBM (176 cm^{-1})	
		Theory, M–B law	Experimental	Theory, M–B law	Experimental
25	300	0.405	0.236	0.368	0.842
100	≈400	≈0.490	0.255	≈0.455	0.860
150	≈450	≈0.523	0.260	≈0.488	0.870
250	≈600	≈0.592	0.275	≈0.562	0.882
Equivalent thermal effect in comparison with the predictions of the M–B law		Cooling		Heating	
Film thickness effect on the I_{aS}/I_S ratio of Raman bands associated with RBM of metallic SWNTs					
$\lambda_{exc} = 676.4$ nm corresponding to the E_{11}^M resonant level excitation of metallic SWNTs 25 mW laser power		I_{aS}/I_S ratio associated with I_{single} of metallic RBM (176 cm^{-1})		I_{aS}/I_S ratio associated with I_{bundle} of metallic RBM (194 cm^{-1})	
		Theory, M–B law	Experimental	Theory, M–B law	Experimental
Thin SWNTs film: ≈60 nm		0.368	0.370	0.355	0.506
Thick SWNTs film: ≈150 m		0.368	0.371	0.355	0.948
Equivalent thermal effect in comparison with the predictions of M–B law		Normal behavior		Heating	

is very sensitive to the variation of the sample temperature. For these, at high temperatures, the values of I_{aS}/I_S tend asymptotically towards 0.86, which is the limit value if the Raman process is governed by the thermal equilibrium rules. Furthermore, figure 4(c) indicates that the I_{aS}/I_S ratio of I_{single} is always greater than the I_{aS}/I_S ratio of I_{bundle}, a fact which seems to contradict the experimental data presented in figures 2 and 3(a).

Table 1 summarizes the essential data regarding the variations of I_{aS}/I_S for Raman bands associated with the RBM components of semiconducting and metallic nanotubes: (i) at $\lambda_{exc} = 1064$ nm as a function of the laser exciting power and (ii) at $\lambda_{exc} = 676.4$ nm as a function of the SWNT film thickness. In the former case, a comparison between the experimental values of the I_{aS}/I_S ratio associated with the two components of the RBM, i.e., I_{single} and I_{bundle}, and those prescribed by the equation (1) evidences opposite deviations, as resulting from a cooling and heating process associated with the nanotubes in the isolated and bundled states, respectively. In this scenario, the cooling effect is understandable as resulting from a supplementary depopulation of the E_{22}^S state by the electronic transition $E_{22}^S \rightarrow E_{11}^S$ followed by luminescence emission at E_{11}^S. Thus, the Raman transitions between the excited and ground E_{22}^S levels occur between vibration states whose populations are no longer described by the M–B law, the above vibration level being partially depleted by phonon relaxation towards the E_{11}^S. The explanation of the heating effect, revealed by a higher value of the I_{aS}/I_S ratio associated with the I_{bundle} component of the RBM, can be obtained by appealing to a CARS process that contributes to the enhancement in all Raman lines on the anti-Stokes side. Such a situation is clearly observable for very different materials at resonant optical excitation when $\chi^{(3)} \neq 0$ [10, 11]. For the metallic nanotubes this occurs at $\lambda_{exc} = 676.4$ nm, when they are resonantly excited at the E_{11}^M state. In this case, because the de-excitation of the E_{11}^M state occurs directly only by spontaneous Raman scattering, I_{single} has a normal behavior in the anti-Stokes side, in accordance with the M–B law. In the complex structure of the RBM, the Raman band associated with I_{bundle} appears enhanced, as resulting from a CARS process. The confirmation of this can be given observing a quadratic dependence of the I_{aS}/I_S ratio both on the sample thickness and on the laser exciting intensity. In our case the former dependence is demonstrated by figure 5 where one sees that at resonant excitation of metallic nanotubes, the intensity of I_{bundle} in the aSR side increases with the SWNT film thickness. As a distinguishing feature we note that the same type of variation is observed for the I_{aS}/I_S ratio adjacent to the G Raman band. The latter dependence is sustained by figure 3(c) where it is shown that I_{bundle} increases two times faster than I_{single}.

Returning to figure 1, it is normal to suppose that the luminescence generated at the E_{11}^S level as a supplementary deactivation path of the E_{22}^S excited level must increase with the laser exciting intensity. In this context, the question arises of whether the complex emission band formed at about 3100 cm^{-1} (figure 3(a)), which changes reversibly with the increase or decrease of the laser excitation intensity within

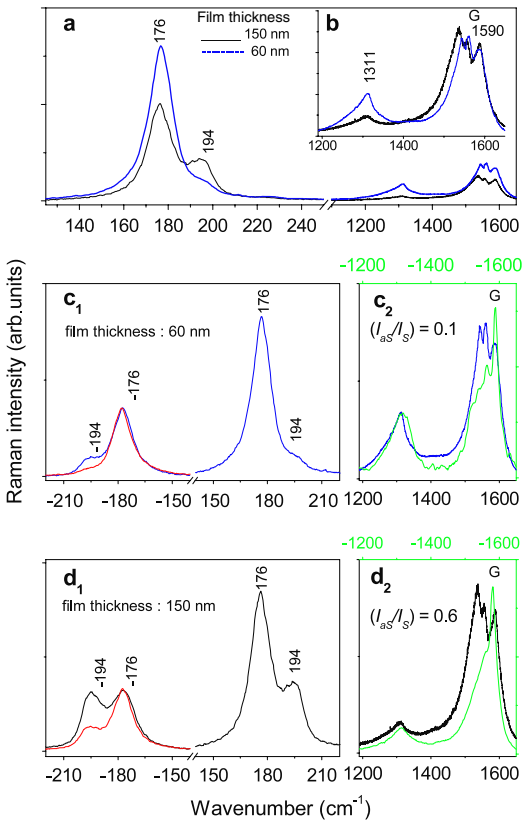

Figure 5. Stokes and anti-Stokes micro-SERS spectra of SWNTs thin films of about 150 nm (black) and 60 nm (blue; shows a greater intensity at -176 cm^{-1}, figure (a)) thickness, at laser ($\lambda_{exc} = 676.4$ nm) power excitation of 25 mW. Using a normalized scale, in (b) we show the Raman spectra covering the interval 1200–1650 cm^{-1} in which the D (1131 cm^{-1}) and G (1590 cm^{-1}) bands are to be found. In (c_1) and (d_1) we detail the Raman spectra recorded on SWNTs thin films of 60 and 150 nm thickness. The red curves, showing a lower intensity for bands at -176 and -174 cm^{-1}, represent the anti-Stokes replica calculated with the equation (1) applied to the Stokes spectra. In (c_2) and (d_2) the green curves show the anti-Stokes Raman spectra associated with the D and G bands. The increase of the intensity ratio (I_{aS}/I_S) of the band G, from 0.1 to 0.6, reveals the operation of a CARS process with a square dependence on the film thickness [11].

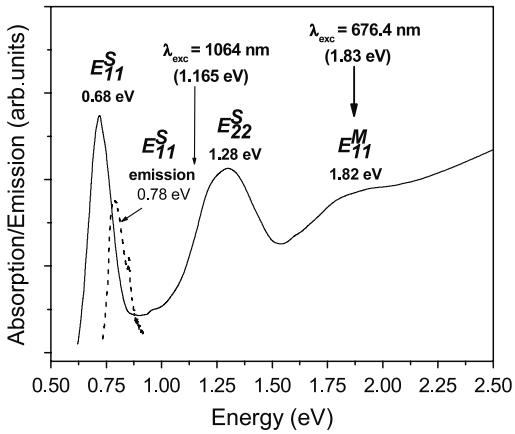

Figure 6. Absorption spectra (full line) of SWNTs used in this paper. The absorption maxima associated with the transitions E_{11}^S, E_{22}^S and E_{11}^M are indicated in the figure. The intense emission band formed in the Raman spectrum at $\sim$3100 cm^{-1} (see figure 3) when the laser ($\lambda_{exc} = 1064$ nm) intensity increases is denoted (dashed curve) as a band with maximum at 0.78 eV.

the 25–250 mW range, may be considered as a luminescence band intrinsically related to the semiconducting nanotubes resonantly excited with 1064 nm or may be ascribed to a compound resulting from the thermal transformation of the nanotubes. In the latter possible scenario, the thermal transformation of nanotubes is expected to be an irreversible process that would result in a new compound which would be gradually developed as the intensity of the laser excitation increases. The presence of such a compound should be observable after performing the first cycle of measurements. However, the presence of such a compound has not been reported to date, therefore invalidating, at least as yet, this hypothesis.

In this context, analyzing table 1, we emphasize that the cooling effect revealed by the lower I_{aS}/I_S ratio of the radial Raman band associated with the isolated nanotubes persists with increased laser excitation light intensity. Observing the absorption spectra of SWNTs used in this work, figure 6, there are three absorption bands, at 0.68, 1.28 and 1.82 eV, which are associated with the transitions from the ground state in the E_{11}^S and E_{22}^S states of semiconducting tubes and the E_{11}^M state of metallic tubes, respectively. On the same graph, the emission band appearing in the Raman spectra at $\sim$3100 cm^{-1} at $\lambda_{exc} = 1064$ nm is shown (figure 3). We are tempted to consider this band, represented by the dashed curve peaking at 0.78 eV, as resulting from the luminescence relaxation of the E_{11}^S excited state populated via the electronic relaxation of the E_{22}^S level; figure 1. The main feature of this band is its nonlinear growth with the exciting laser intensity; figure 3(c). Such a variation is not surprising; it is similar to the change in intrinsic luminescence of any direct gap semiconductor when a thermal matching of the band gap with the laser exciting energy occurs. In our case, the increase in the sample temperature caused by the increase of the exciting laser intensity reduces the separation of the E_{22}^S and E_{11}^S energy levels. In this way the depletion of the former level by the phonon transition $E_{22}^S \rightarrow E_{11}^S$ is facilitated. The deactivation of the latter level explains the enhancement of the intrinsic luminescence marked in figure 3(a) by the intense band at $\sim$3100 cm^{-1}. The reasoning developed here remains valuable despite the fact that the emission band at $\sim$3100 cm^{-1} in figure 3 indicated by the dashed line in figure 6 is certainly truncated on its low energy side by the technical limit of the Raman spectrophotometer used, whose Stokes interval is limited at $\sim$3500 cm^{-1}.

In accordance with other reported data, the matching of position and profile between E_{11}^S absorption and luminescence bands of SWNTs [13] is taken as an argument for the emission band at 3100 cm^{-1} originating in the radiative de-excitation of the E_{11}^S level associated with the isolated semiconducting nanotubes. Other experimental results corroborate this statement. In this sense we find it sufficient to note that at $\lambda_{exc} = 676.4$ nm, when the metallic nanotubes are resonantly excited, any luminescence growing with increased exciting laser intensity is absent.

4. Conclusions

Summarizing all the above we notice that: (i) the Raman process of the semiconducting SWNT, under resonant excitation at 1064 nm, when the E_{22}^{S} transition is activated, evolves in conditions of non-thermal equilibrium similarly to a quantum cooling process; (ii) this is due to a supplementary depletion of the upper excited state E_{22}^{S} by the electronic transition towards the excited E_{11}^{S} state and thereafter by luminescence emission in the ground state; (iii) the cooling effect is detected by a smaller value of the anti-Stokes/Stokes Raman intensity ratio (I_{aS}/I_{S}) associated with the radial breathing vibration modes of isolated nanotubes; (iv) a supplementary a heating effect revealed by an increased value of the (I_{aS}/I_{S}) ratio associated with the RBM of bundled tubes is attributed to a CARS process; (v) the vibration cooling effect is no longer observed when the metallic tubes are resonantly excited at E_{11}^{M}. This is corroborated by the fact that the metallic nanotubes are not luminescent.

Acknowledgments

This work has been performed in the framework of the Scientific Cooperation between the Institute of Materials in Nantes and the Laboratory of Optics and Spectroscopy of the National Institute of Materials Physics in Bucharest. This research was financed by the Romanian National University Research Council as an IDEAS project No 41/2007.

References

[1] Dresselhauss M S and Eklund P C 2000 *Adv. Phys.* **49** 705
[2] Dresselhaus M S, Dresselhaus G, Jorio A, Souza Filho A G and Saito R 2002 *Carbon* **42** 2043–61 and references therein
[3] Dresselhaus M S, Dresselhaus G, Saito R and Jorio A 2005 *Phys. Rep.* **409** 47–99 and references therein
[4] Bandow S, Asaka S, Saito Y, Rao A M, Grigorian L, Richter E and Eklund P C 1998 *Phys. Rev. Lett.* **80** 3779–82
[5] Rao A M, Chen J, Richter E, Schlecht U, Eklund P C, Haddon R C, Venkateswaran U D K, Kwon Y K and Tomanek D 2001 *Phys. Rev. Lett.* **86** 3895–8
[6] Brown S D M, Corio P, Marucci A, Dresselhauss M S, Pimenta M A and Kneipp K 2000 *Phys. Rev.* B **61** R5137–40
[7] Kneipp K, Kneipp H, Corio P, Brown S D M, Shafer K, Motz J, Perelman L T, Hanlon E B, Marucci A, Dresselhauss G and Dresselhauss M S 2000 *Phys. Rev. Lett.* **84** 3470–3
[8] Thomsen C and Reich S 2000 *Phys. Rev. Lett.* **85** 5214–7
[9] Kneipp K, Wang Y, Kneipp H, Itzkan I, Dasari R R and Feld M S 1996 *Phys. Rev. Lett.* **76** 2444–7
[10] Baltog I, Baibarac M and Lefrant S 2005 *J. Opt. A: Pure Appl. Opt.* **7** 632–9
[11] Baltog I, Baibarac M and Lefrant S 2005 *Phys. Rev.* B **72** 245402–11
[12] Rousseau D L, Fiedeman J M and Williams P F 1979 *Raman Spectroscopy of Gases and Liquids* (*Springer Topics in Current Physics* vol 11) ed A Weber (Berlin: Springer) chapter 6
[13] Bachilo S M, Strano M S, Kitrell C, Hauge R H, Smalley R E and Weisman R B 2002 *Science* **298** 2361–6
[14] Epstein R I, Buchwald M I, Edwards B C, Gosnell T R and Mungan C E 1995 *Nature* **377** 500–3
[15] Rupper G, Kwong N H and Bidner R 2006 *Phys. Rev. Lett.* **97** 117401
[16] Journet C, Maser W K, Bernier P, Loiseau A, Lamy de la Chapelle M, Lefrant S, Lee R and Fisher J E 1997 *Nature* **388** 756–8
[17] Vaccarini L, Goze C, Aznar R, Micholet V, Journet C and Bernier P 1999 *Synth. Met.* **103** 2492–3
[18] Lefrant S, Baltog I and Baibarac M 2005 *J. Raman Spectrosc.* **36** 676–98
[19] Zhou Z, Dou X, Ci L, Song L, Liu D, Gao Y, Wang J, Liu L, Zhou W, Xie S and Wan D 2006 *J. Phys. Chem.* B **110** 1206–9
[20] Cronin S B, Yin Y, Walsh A, Capaz R B, Stolyarov A, Tangney P, Cohen M L, Louie S G, Swan A K, Unlu M S, Goldberg B B and Tinkham M 2006 *Phys. Rev. Lett.* **96** 127403-1–4
[21] Ouayang Y and Fang Y 2004 *Physica* E **24** 222–6